Sigma-Bond-to-Ligand Charge Transfer Transitions and Excited States of d6 Metal-Diimine Complexes.

van Slageren, J.

Publication date
2000

CHAPTER

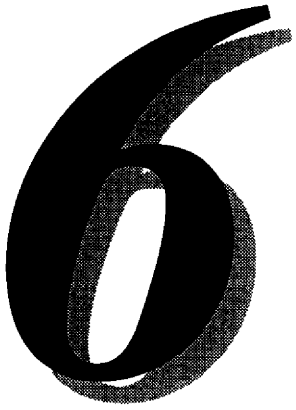

The Complexes cis-[Rh(R)$_2$(I)(CO)(dmb)] (R = Me, iPr; dmb = 4,4'-dimethyl-2,2'-bipyridine): Synthesis, Structure and Photoreactivity

Van Slageren, J.; Vermeer, A.L.; Stufkens, D.J., Lutz, M.; Spek, A.L., submitted to *J. Organomet. Chem.*

6.1 Abstract

In this chapter the synthesis, structure and photochemistry of the novel rhodium(III) complexes *cis*-[Rh(R)$_2$(I)(CO)(dmb)] (R = Me (**1**), iPr (**2**)) are described. Although many di- and trimethyl–rhodium(III) complexes are known, *cis*-[Rh(iPr)$_2$(I)(CO)(dmb)] (**2**) is the first diisopropyl–rhodium(III) compound. Single crystal X-Ray diffraction studies revealed the structure of **1**. The lowest electronic transition has Halide-to-Ligand Charge Transfer character according to resonance Raman spectra, obtained by excitation into the corresponding absorption band. Upon irradiation in solution, both **1** and **2** give rise to Rh–R bond homolysis as evidenced by spin-trap EPR investigations. The photoreaction occurs after crossing to the reactive Sigma-Bond-to-Ligand Charge Transfer (SBLCT) state. For the iPr-complex homolysis is observed at longer wavelength irradiation than for the methyl derivative, indicating that in the former case the SBLCT-state is lower in energy.

6.2 Introduction

Complexes with a lowest Metal-to-Ligand Charge Transfer (MLCT) state, such as [Ru(bpy)$_3$]$^{2+}$and [Re(Cl)(CO)$_3$(bpy)] have been extensively studied with regard to their excited state properties. By replacement of the chloride in the latter complex by a strongly σ donating ligand L, such as an alkyl group or metal fragment, σ(Re–L) of [Re(L)(CO)$_3$(α-diimine)] may become the HOMO. As a result, the lowest excited state obtains Sigma-Bond-to-Ligand Charge Transfer (SBLCT) character.[1,2] The photochemical properties of the complexes [Re(L)(CO)$_3$(α-diimine)] have been studied extensively in our laboratory.[3–5] It was found that occupation of the SBLCT excited state can give rise to efficient Re–L bond homolysis. Later these studies were extended to [M(L$_1$)(L$_2$)(CO)$_2$(α-diimine)] (M = Ru, Os) and [Pt(L)$_2$(Me)$_2$(α-diimine)].[6–8] However, not many complexes are known from group 9, in which low lying SBLCT states are present. One well studied example is vitamin B12 and its model complexes,[9] for which the SBLCT excited state was proposed to be responsible for the observed Co–C bond splitting.[10] Apart from these examples, to our knowledge the only group 9 organometallic complexes shown to possess such SBLCT excited states are *fac*-[Ir(III){tris-(6-isopropyl-8-quinolyl)diorganosilyl}],[11,12] and [Ir(R)(CO)(PPh$_3$)$_2$(mnt)] (R = Me, Et; mnt = maleonitriledithiolate).[13]

Here we present the synthesis, structure and photochemistry of two novel complexes [Rh(R)$_2$(I)(CO)(dmb)] (R = Me (**1**), iPr (**2**); dmb = 4,4'-dimethyl-2,2'-bipyridine).

6.3 Experimental Section

Materials. I_2 (Merck), 4,4'-dimethyl-2,2'-bipyridine (dmb, Fluka), MeMgCl (3.0 M in THF, Aldrich), iPrMgCl (2.0 M in THF, Aldrich), $AgNO_3$ (Aldrich, 99%) were used as received. Solvents purchased from Acros (THF, hexane, pentane, dichloromethane, acetonitrile, diethyl ether, methanol, 2-MeTHF) were dried on and distilled from the appropriate drying agent when necessary. Silica gel (kieselgel 60, Merck, 70–230 mesh) for column chromatography was dried and activated by heating *in vacuo* at 160 °C overnight.

Syntheses. All syntheses were performed under a nitrogen atmosphere using standard Schlenk techniques. [Rh(Cl)(CO)$_2$]$_2$ [14] was prepared according to a literature procedure.

[Rh(Cl)(CO)(dmb)]. To a solution of [Rh(Cl)(CO)$_2$]$_2$ in THF, 1.1 eq dmb in THF was added at –78 °C. The reaction mixture was allowed to warm to room temperature while stirring. Evaporation of the solvent and washing with hexane afforded the red product as a solid in *ca.* 90% yield. IR (THF); ν(CO) : 1970 cm^{-1}. UV (THF); λ_{max}: 501 nm. ^{1}H NMR ($CDCl_3$); δ : 2.42 (s, 6H, dmb CH_3), 2.54, (s, 6H, dmb CH_3), 7.04 (d, ^3J = 5.6 Hz, 2H, dmb H5), 7.29 (d, ^3J = 5.9 Hz, 2H, dmb H5), 7.76 (s, 1H, dmb H3), 7.80 (s, 1H, dmb H3), 8.51 (d, ^3J = 5.6 Hz, 2H, dmb H6), 9.16 (d, ^3J = 5.8 Hz, 2H, dmb H6) ppm.

[Rh(NO$_3$)(CO)(dmb)]. A suspension of exactly one equivalent of $AgNO_3$ in a solution of 150 mg [Rh(Cl)(CO)(dmb)] in THF was stirred overnight at room temperature. Filtration and evaporation of the solvent gave the red product in near quantitative yield. IR (THF) ; ν(CO) : 1970 cm^{-1}. ^{1}H NMR ($CDCl_3$); δ : 2.42 (6H, dmb CH_3), 2.54, (6H, dmb CH_3), 7.04 (2H, dmb H5), 7.29 (2H, dmb H5), 7.76 (1H, dmb H3), 7.80 (1H, dmb H3), 8.51 (2H, dmb H6), 9.16 (2H, dmb H6) ppm.

[Rh(I)$_2$(NO$_3$)(CO)(dmb)]. Dropwise addition of one equivalent of I_2 in THF to a solution of 100 mg [Rh(NO$_3$)(CO)(dmb)] in THF at –78 °C, overnight stirring at room temperature and subsequent evaporation of the solvent yielded the crude product. Washing with pentane gave the pure orange-brown product in *ca.* 80% yield. IR (THF) ; ν(CO) : 2098 cm^{-1}. ^{1}H NMR ($CDCl_3$); δ : 2.64 (s, 6H, dmb CH_3), 2.68 (s, 6H, dmb CH_3), 7.35 (d, ^3J = 5.8 Hz, 2H, dmb H5), 7.55 (d, ^3J = 6.3 Hz, 2H, dmb H5), 7.99 (s, 2H, dmb H3), 8.66 (d, ^3J = 6.0 Hz, 2H, dmb H6), 9.69 (d, ^3J = 5.9 Hz, 2H, dmb H6) ppm.

***cis*-[Rh(Me)$_2$(I)(CO)(dmb)] (1).** To a solution of [Rh(I)$_2$(NO$_3$)(CO)(dmb)] (100 mg) in THF at –78 °C, two equivalents of MeMgCl (3.0 M in THF) were gradually added through a syringe, while following the reaction by IR. The colour of the reaction mixture changed from brown to brown-red

during the addition. The solid obtained after quenching of the excess of Grignard and evaporation of the solvent in vacuo, was dissolved in CH_2Cl_2 and washed repeatedly with water. Drying on anhydrous $MgSO_4$ and evaporation of the solvent yielded the crude product which was purified by column chromatography (activated silica, CH_2Cl_2/hexane gradient elution) and obtained as a yellow-brown solid in *ca.* 50 % yield. FAB-MS; *m/z*: [M^+] not detected, 817 [$2M^+ - I$] (resulting from gas phase clustering), 787 [$2M^+ - I - 2$ Me], 457 [$M^+ -$ Me], 345 [$M^+ - I$], 315 [$M^+ - 2$ Me $- I$], 287 [$M^+ - 2$ Me $- I -$ CO]. IR (THF) ; ν(CO) : 2031 cm^{-1}. UV (THF); λ_{max}: 295, 370 nm. ^{1}H NMR (CD_2Cl_2); δ : 0.54 (d, J_{Rh-H} = 2.2 Hz, 3H, Rh–Me_{ax}, assignment corresponding to [15]), 1.18 (d, J_{Rh-H} = 2.0 Hz, 3H, Rh–Me_{eq}), 2.53, (s, 3H, dmb CH_3), 7.33 (d, ^3J = 5.6 Hz, 2H, dmb H5), 7.42 (d, ^3J = 5.3 Hz, 2H, dmb H5), 8.07 (s, 2H, dmb H3), 8.76 (d, ^3J = 5.6 Hz, 2H, dmb H6), 8.77 (d, ^3J = 5.3 Hz, 2H, dmb H6) ppm. ^{13}C NMR APT (CD_2Cl_2): δ –0.9 (d, J_{Rh-C} = 22 Hz, Rh–Me_{ax}), 6.6 (d, J_{Rh-C} = 22 Hz, Rh–Me_{eq}), 21.4 (dmb Me), 123.7 (dmb C3), 123.9 (dmb C3), 127.3 (dmb C5), 127.7 (dmb C5), 147.7 (dmb C6), 151.4 (dmb C6), 150.6 (dmb C4), 151.5 (dmb C4), 152.7 (dmb C2), 155.2 (dmb C2), 191.3 (J_{Rh-C} = 68 Hz, CO) ppm.

***cis*-[Rh(iPr)$_2$(I)(CO)(dmb)] (2).** This complex was synthesized by reaction of [Rh(I)$_2$(NO_3)(CO)(dmb)] (100 mg) and two equivalents of iPrMgCl in Et_2O using the same method as for [Rh(Me)$_2$(NO_3)(CO)(dmb)]. The reaction product was purified by pentane extraction of the solid obtained after quenching and evaporation of the solvent. The orange-brown product was obtained in 80% yield. FAB-MS; *m/z*: [M^+] not detected, 929 [$2\ M^+ - I$] (resulting from gas phase clustering), 843 [$2\ M^+ - I -$ 2 iPr], 729 [$2\ M^+ - I -$ 4 iPr – CO], 701 [$2\ M^+ - I -$ 4 iPr – 2 CO], 401 [$M^+ - I$], 315 [$M^+ -$ 2 Me $- I$], 287 [$M^+ - 2$ Me $- I -$ CO]. IR (THF) ; ν(CO) : 2021 cm^{-1}. UV (THF); λ_{max}: 295, 370 nm. ^{1}H NMR (CD_2Cl_2); δ : 0.72 (pst, $^3J \approx J_{Rh-H} \approx$ 6.3 Hz, 3M, Rh–CH(CH_3)$_2$), 0.92 (m, 1H, Rh–C*H*(CH_3)$_2$ (ax, assignment corresponding to [15])), 1.09 (pst, $^3J \approx J_{Rh-H} \approx$ 6.3 Hz, 3H, Rh–CH(CH_3)$_2$), 1.24 (m, 3H, Rh–CH(CH_3)$_2$, 1.7 (m, 3H, Rh–CH(CH_3)$_2$), 2.09 (m, 1H, Rh–C*H*(CH_3)$_2$ (eq)), 2.52 (s, 3H, dmb CH_3), 2.58 (s, 3H, dmb CH_3), 7.36 (d, ^3J = 5.4 Hz, 1H, dmb H5), 7.43 (d, ^3J = 5.1 Hz, 1H, dmb H5), 8.02 (s, 2H, dmb H3), 8.61 (d, ^3J = 6.0 Hz, 2H, dmb H6), 8.76 (d, ^3J = 5.4 Hz, 2H, dmb H6) ppm. ^{13}C NMR APT (CD_2Cl_2); δ : 16.9 (d, J_{Rh-C} = 2.8 Hz, Rh–CH(CH_3)$_2$), 18.8 (d, J_{Rh-C} = 2.6 Hz, Rh–CH(CH_3)$_2$), 21.5 (dmb Me), 27.3 (Rh–CH(CH_3)$_2$), 30.4 (Rh–CH(CH_3)$_2$), 31.7 (J_{Rh-C} = 22 Hz, Rh–C*H*(CH_3)$_2$), 33.7 (J_{Rh-C} = 23 Hz, Rh–C*H*(CH_3)$_2$), 123.6 (dmb C3), 123.9 (dmb C3), 127.2 (dmb C5), 127.5 (dmb C5), 147.2 (dmb C6), 150.4 (dmb C4), 151.0 (dmb C6), 151.5 (dmb C4), 152.6 (dmb C2), 155.5 (dmb C2), 193.1 (J_{Rh-C} = 73 Hz, CO) ppm.

Measurements. FAB$^+$-MS spectra were obtained on a JEOL JMS SX/SX102A four-sector mass spectrometer coupled to a JEOL MS-MP7000 data system. Infrared spectra were recorded on Bio-Rad FTS-7 and FTS-60A FTIR spectrophotometers (the latter equipped with a liquid-nitrogen-cooled MCT detector), and electronic absorption spectra on Varian Cary 4E and Hewlett-Packard 8453 spectrophotometers. NMR spectra were recorded on a Varian Mercury 300 (300.13 MHz and

75.46 MHz for ^{1}H and ^{13}C, respectively) spectrometer. Resonance Raman spectra of the complexes dispersed in KNO_3 pellets were recorded on a Dilor XY spectrometer equipped with a Wright Instruments CCD detector, using a Spectra Physics 2040E Ar^+ laser as the excitation source. EPR spectra were recorded using a Varian E-104A instrument. The radicals were generated by *in situ* irradiation using an Oriel high pressure mercury lamp.

Single-crystal structure determination of 1. Suitable crystals of **1** were grown by vapour diffusion of hexane into a solution of 1 in CH_2Cl_2 at –20 °C. Crystal data: $C_{15}H_{18}IN_2ORh{\cdot}CH_2Cl_2$, FW = 557.05, colourless block, 0.36 × 0.27 × 0.12 mm^3, monoclinic, $P2_1/c$ (No. 14), a = 11.0746(3) Å, b = 14.1766(4) Å, c = 14.5336(4) Å, β = 119.462(2)°, V = 1986.70(10) Å^3, Z = 4, ρ = 1.862 g cm^{-1}. Intensities were measured on a Nonius KappaCCD diffractometer, with rotating anode (Mo-K_α, λ = 0.71073Å) at 150 K. The absorption correction was based on multiple measured reflections (PLATON[16], μ = 2.69 mm^{-1}, 0.63–0.71 transmission). 17229 measured reflections, 4538 unique reflections (R_{int} = 0.0553). The structure was solved with direct methods (SIR-97[17]) and refined with the program SHELXL-97[18] against F^2 of all reflections up to a resolution of $(\sin \theta/\lambda)_{max}$ = 0.65 Å^{-1}. The two equatorial ligand positions are partially occupied by methyl and carbonyl groups, respectively. The carbon atoms were not split and refined with an occupancy of 1. For the carbonyl oxygen and the methyl hydrogens the occupancy was refined under the assumption that the total occupancy is 1. The refinement resulted in a disorder ratio of 0.677(7):0.323(7). Non hydrogen atoms were refined freely with anisotropic displacement parameters. Hydrogen atoms were refined as rigid groups. 221 parameters. The drawing, calculations and checking for higher symmetry were performed with the PLATON[16] package. R(I>2σ(I)): R1 = 0.0275, wR2 = 0.0635. R (all data): R1 = 0.0332, wR2 = 0.0654. S = 1.102.

Crystallographic data (excluding structure factors) for the structure in this chapter have been deposited with the Cambridge Crystallographic Data Centre as supplementary publication no. CCDC 150426. Copies of the data can be obtained, free of charge, on application to CCDC, 12 Union Road, Cambridge CB2 1EZ, UK (fax: +44-1223 336033 or e-mail: deposit@ccdc.cam.ac.uk).

6.4 Results and Discussion

6.4.1 Syntheses

The synthesis of [Rh(Cl)(CO)(α-diimine)] from $[Rh(Cl)(CO)_2]_2$ was shown to proceed by α-diimine coordination resulting in $[Rh(Cl)(CO)_2$(α-diimine)], prior to CO loss.[19] This pentacoordinated complex may dissociate into an $[Rh(CO)_2$(α-diimine)$]^+(Cl)^-$ ion pair.[20]

These intermediates were isolated in several cases.[21-23] The synthesis of [Rh(Cl)(CO)(dmb)] (dmb = 4,4'-dimethyl-2,2'-bipyridine) did not yield such species. Thus, the product obtained was red in accordance with the observed colour for [Rh(Cl)(CO)(bpy)],[24] whereas *e.g.* [Rh(CO)$_2$(phen)]$^+$(ClO$_4$)$^-$ was reported to be green.[22] Moreover, only one band due to ν(CO) was found in the IR spectrum at 1970 cm^{-1} in THF, in correspondence with literature data for [Rh(Cl)(CO)(bpy)] (1977 cm^{-1} in MeCN).[25] In addition, ^{1}H NMR showed the dmb ligand to be in an asymmetric environment, which is not the case for [Rh(CO)$_2$(α-diimine)]$^+$(Cl)$^-$.

Apart from these products, in the reaction of [Rh(Cl)(CO)$_2$]$_2$ with an α-diimine ligand afforded [Rh(CO)$_2$(Cl)$_2$]$^-$ [Rh(CO)$_2$(α-diimine)]$^+$ ion pairs,[22,23] especially when an excess of [Rh(Cl)(CO)$_2$]$_2$ was used. Our synthetic procedure did not give rise to such species.

When [Rh(Cl)(CO)(dmb)] was allowed to react with one equivalent of I$_2$, a mixture of two products was formed, in both of which the dmb ligand is in an asymmetric environment according to ^{1}H NMR. Since removal of the chloride ligand, using AgNO$_3$, prior to oxidative addition of I$_2$ was found to result in a single, pure product, the products of the reaction of [Rh(Cl)(CO)(dmb)] with I$_2$ were not investigated further. NMR showed that the two pyridyl rings of the dmb ligand of [Rh(I)$_2$(NO$_3$)(CO)(dmb)] are unequal.

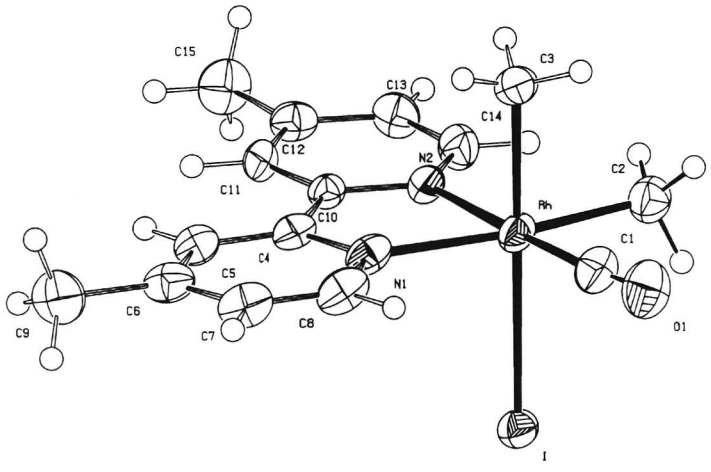

Figure 6.1 Displacement ellipsoid plot of **1** (50% probability level). The CH_2Cl_2 molecule, present in the asymmetric unit, has been omitted for clarity. The methyl and carbonyl groups in the equatorial plane are disordered: The ligand position at C1 consists of 67.7(7)% carbonyl and 32.3(7)% methyl; the ligand position at C2 *vice versa*.

Gradual addition of MeMgCl to [Rh(I)$_2$(NO$_3$)(CO)(dmb)] caused the IR band due to the starting compound (2098 cm^{-1}) to disappear, while initially a band at 2058 cm^{-1} appeared which was in turn replaced by one at 2031 cm^{-1}. This indicates successive addition of two methyl groups. Single crystal X-Ray diffraction studies (*vide infra*) revealed the structure to be that depicted in Figure 6.1.

Addition of iPrMgCl to [Rh(I)$_2$(NO$_3$)(CO)(dmb)] gave the corresponding orange-brown diisopropyl–rhodium species [Rh(iPr)$_2$(I)(CO)(dmb)] (**2**) The ν(CO) vibration has shifted to lower wavenumbers (2021 cm^{-1}), in line with the higher σ-donating strength of the isopropyl group, compared to the methyl ligand. Although Rh–iPr complexes are known,[26–29] **2** is to our knowledge the first diisopropyl–rhodium complex. Table 6.1 presents all vibrational (IR, resonance Raman) data for complexes **1** and **2**.

Table 6.1 Vibrational data for complexes **1** and **2**.

Compound	IR[a] ν(CO)[b]	resonance Raman[c] (cm^{-1})
[Rh(Me)$_2$(I)(CO)(dmb)] (**1**)	2031	1621, 1560, 1492, 1322, 1284, 1030, 564, 526
[Rh(iPr)$_2$(I)(CO)(dmb)] (**2**)	2021	1621, 1560, 1492, 1326, 1276, 1033, 570, 523, 234
dmb	–	1606, 1561, 1486, 1315, 1290, 1034, 236[d]

[a]in THF at room temperature; [b]in cm^{-1}; [c]in KNO$_3$; [d]selected Raman bands observed on 514.5 nm excitation of the ligand dispersed in a KNO$_3$ pellet.

6.4.2 Crystal structure of *cis*-[Rh(Me)$_2$(I)(CO)(dmb)] (1)

Table 6.2 lists the most important bond lengths and angles of **1**, while Figure 6.1 shows a molecular The coordination environmentof the Rh centre is distorted octahedral. The equatorial positions are occupied by the dmb ligand, a methyl and a carbonyl group, while an iodide and methyl group are in the axial ones. The dmb ligand is essentially planar with N–Rh bond lengths of 2.124(2) and 2.144(3) Å. The N–Rh–N angle of 76.76(9)° is significantly smaller than the perfect octahedral angle of 90°. The Rh–I bond length (2.7936(3) Å) is similar to that in [Rh(Cl)(I)(CH$_2$I)(CO)(PEt$_3$)$_2$] (2.803 Å),[30] and also to that of the iso-electronic complexes *trans*, *cis*-[Ru(I)(CH$_3$)(CO)$_2$(iPr–DAB)] (2.7998(9) Å),[31] but slightly shorter than that of [Pd(I)(Me)$_3$(bpy)] (2.834 Å).[32] The axial Rh–CH$_3$ bond (2.102(3) Å) is significantly longer than the equatorial ones (1.933(4) and 2.014(3) Å), indicating that the axial Rh–CH$_3$ bond is weaker (for the methyl carbonyl disorder, see section 6.3). A similar situation was encountered for [Pt(Me)$_4$(cHx–DAB)] where the axial and equatorial Pt–C bond lengths are 2.140(8) Å and 2.045(5) Å, respectively.[15] In contrast, for [Pd(I)(Me)$_3$(bpy)], the

axial and equatorial Pd–C bond lengths are similar (2.040 Å and 2.034/2.046 Å, respectively).[32]

Table 6.2 Important bond lengths (Å) and angles (°) of non-hydrogen atoms of **1**. Esd in last digit in parentheses.

Bond	Length (Å)	Bonds	Angle (°)
Rh–I	2.7936(3)	I–Rh–N1	89.86
Rh–C1	1.933(5)	I–Rh–N2	90.93
Rh–C2	2.014(3)	I–Rh–C1	92.20
Rh–C3	2.103(4)	I–Rh–C2	92.87
Rh–N1	2.144(2)	I–Rh–C3	179.56
Rh–N2	2.124(3)	N1–Rh–C1	101.54
		C1–Rh–C2	84.94
Dmb	Torsion Angle (°)	N2–Rh–C2	96.61
N1–C4–C10–N2	1.0(4)	N1–Rh–N2	76.76

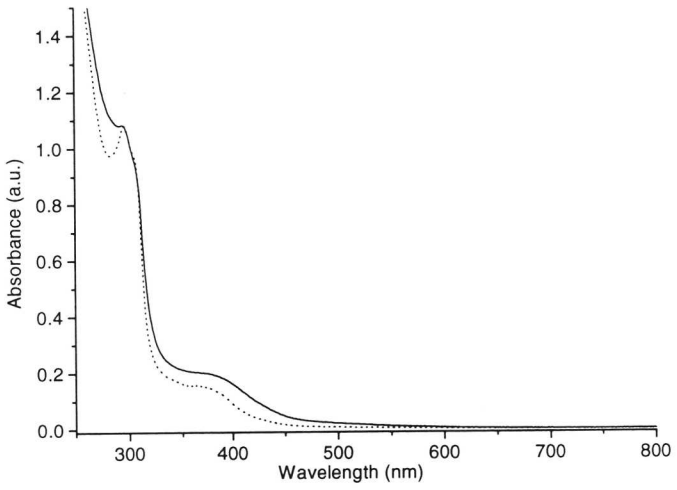

Figure 6.2 Absorption spectra of **1** (dotted) and **2** (drawn) in THF.

6.4.3 Electronic absorption and resonance Raman (rR) spectra

Figure 6.2 depicts the absorption spectra of **1** and **2** in THF. The spectra of both complexes show the dmb intraligand band at 295 nm as well as an absorption band at *ca.* 370 nm. The negative solvatochromism ($\Delta\nu = \nu$(MeCN) – ν(toluene) $\approx 2.2 \times 10^3$ cm^{-1}) indicates that the transition belonging to the lowest-energy absorption band has strong charge transfer

character. In order to characterize these electronic transitions, rR spectra were recorded by excitation into these bands (Figure 6.3, Table 6.1).

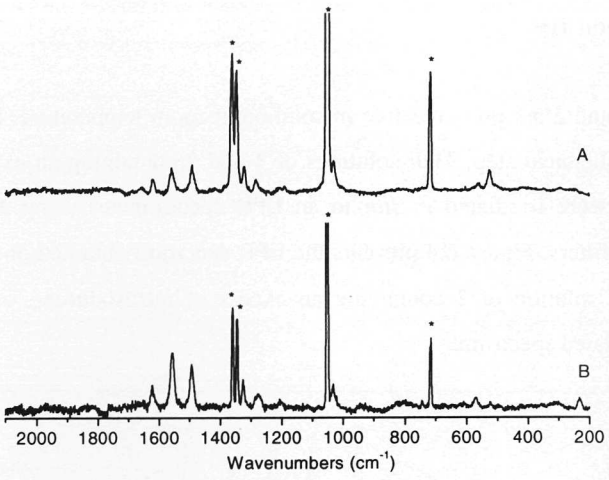

Figure 6.3 Resonance Raman spectra of (A) **1** (λ_{exc} = 457.9 nm) at room temperature and (B) **2** (λ_{exc} = 457.9 nm) at 90K in KNO_3. Asterisks denote nitrate bands.

The merit of the rR technique is based on the fact that those vibrations show a high Raman intensity that are coupled to the allowed electronic transition which is excited.[33] For comparison, the Raman spectrum of the free ligand was recorded under the same conditions. The resonance enhanced vibrations for both **1** and **2** can all be assigned to dmb ligand vibrations, although the intensities of the resonance Raman bands of the complexes differ from those of the free ligand. This difference is due to the fact that in resonance Raman the intensity of a particular band is determined by the distortion of the compound in the excited state along the normal coordinate of that vibration, whereas the change in polarizability determines the intensity of a normal Raman band. The observation of resonance enhanced dmb vibrations implies the involvement of this ligand in the electronic transition belonging to the absorption band into which excitation takes place. The CO stretching frequency is not resonance enhanced, which implies that the charge density on the central metal atom is not affected by the electronic transition hence ruling out an MLCT assignment. No alkyl ligand vibrations are resonance enhanced which makes Sigma-Bond-to-Ligand Charge Transfer (SBLCT) character unlikely. Taking this into account, the lowest-energy absorption band most probably belongs to a Halide-to-Ligand Charge Transfer XLCT (X = I) transition. A

similar character of the lowest-energy electronic transition was found for [Re(I)(CO)$_3$(α-diimine)],[34] [Ru(I)(Me)(CO)$_2$(α-diimine)],[31] and [Pt(I)(Me)$_3$(iPr–DAB)].[7]

6.4.4 Photochemistry

Both **1** and **2** are photoreactive in solution at room temperature. In order to study the primary photochemical step, THF solutions of **1** and **2** containing an excess of the spin-trap nitrosodurene, were irradiated *in situ* in an EPR spectrometer using a mercury lamp and suitable cutoff filters. Figure 6.4 presents the EPR spectrum obtained on irradiation (λ_{irr}>435 nm) of a THF solution of **2** containing an excess of nitrosodurene, as well as the PEST Winsim[35] simulated spectrum.

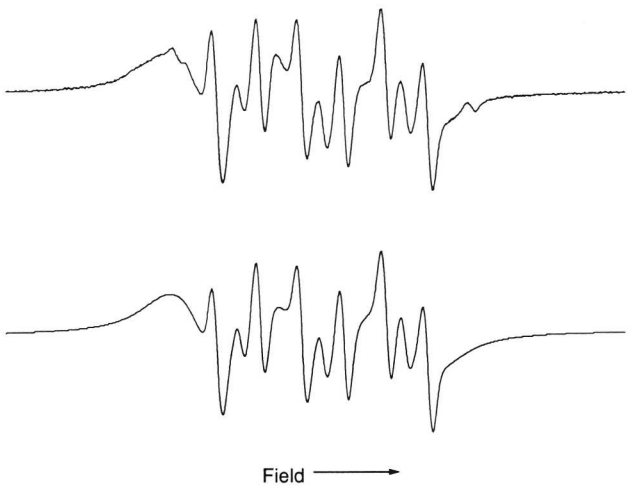

Figure 6.4 Experimental (top) and simulated (bottom) EPR spectra obtained on irradiation (λ_{irr}>435) of **2** in a THF solution containing an excess of nitrosodurene.

The complicated spectrum indicates that both the metal fragment radical and the alkyl radical are trapped by nitrosodurene. Irradiation in the presence of an excess of PPh_3, used previously to trap the metal fragment selectively,[36] did not result in any observable EPR signal. The best fit is obtained by assuming the presence of a small amount of a third EPR active species (probably free nitrosodurene radical), in addition to the nitrosodurene (nd) trapped isopropyl and metal fragment radicals. The hyperfine splitting constants for nd–iPr$^{\bullet}$ derived from the fitting procedure are a_N = 13.59 G and a_H = 6.80 G, in agreement with

literature values of 13.8 G and 6.7 G, respectively.[37] The fitted hyperfine constants for the nd trapped metal fragment are a_N = 16.66 G (nd), a_{Rh} = 1.19 G and a_N = 2.16 G (dmb). Due to the large linewidth of the latter radical (5.8 G) these last two splitting constant values are not very reliable. The fact that these values are small indicates that the electron spin is mainly located on the nd nitrogen atom.

Complex **1** does not show any radical formation under these circumstances, but shorter wavelength irradiation (λ_{irr}>335 nm) does give rise to EPR detectable signals. In all cases, the photochemical reaction is not very efficient, with estimated quantum yields less than 0.01. On lowering the temperature, the efficiency is even much lower.

An XLCT excited state generally does not result in photochemical bond homolysis. Hence, the observed photoreaction must occur after crossing from the optically occupied electronic state to a reactive one. Of the excited states known to give rise to bond homolysis, the SBLCT state is the most likely candidate. Similar XLCT to SBLCT crossings were found for [Ru(I)(R)(CO)$_2$(iPr–DAB)] (R = iPr, Bz).[38,39] In general, the energy of the transition metal to carbon bond of a metal–alkyl complex increases with increasing σ donor strength of the alkyl group, decreasing the energy of the SBLCT-state. In the complexes under study, the iPr group is the stronger σ donor. This explains that radical formation occurs at lower-energy irradiation for **2** than in the case of **1**.

6.5 References

1) Morse, D. L.; Wrighton, M. S. *J. Am. Chem. Soc.* **1976**, *98*, 3931.

2) Luong, J. C.; Faltynek, R. A.; Wrighton, M. S. *J. Am. Chem. Soc.* **1980**, *102*, 7892.

3) Stufkens, D. J. *Comments Inorg. Chem.* **1992**, *13*, 359.

4) Rossenaar, B. D.; Kleverlaan, C. J.; van de Ven, M. C. E.; Stufkens, D. J.; Vlček, Jr., A. *Chem. Eur. J.* **1996**, *2*, 228.

5) Rossenaar, B. D.; Lindsay, E.; Stufkens, D. J.; Vlček, Jr., A. *Inorg. Chim. Acta* **1996**, *250*, 5.

6) Aarnts, M. P.; Stufkens, D. J.; Wilms, M. P.; Baerends, E. J.; Vlček, Jr., A.; Clark, I. P.; George, M. W.; Turner, J. J. *Chem. Eur. J.* **1996**, *2*, 1556.

7) van Slageren, J.; Záliš, S.; Klein, A.; Stufkens, D. J. submitted to *Inorg. Chem.*.; chapter 7.

8) van Slageren, J.; Stufkens, D. J. submitted to *Inorg. Chem.*; chapter 3.

9) Shiang, J. J.; Walker, II, L. A.; Anderson, N. A.; Cole, A. G.; Sension, R. J. *J. Phys. Chem. B* **1999**, *103*, 10532.

10) Kunkely, H.; Vogler, A. J. *J. Organomet. Chem.* **1993**, *453*, 269.

11) Djurovich, P. I.; Watts, R. J. *Inorg. Chem.* **1993**, *32*, 4681.

12) Djurovich, P. I.; Watts, R. J. *J. Phys. Chem.* **1994**, *98*, 396.

13) Bradley, P.; Suardi, G.; Zipp, A. P.; Eisenberg, R. *J. Am. Chem. Soc.* **1994**, *116*, 2859.

14) McCleverty, J. A.; Wilkinson, G. *Inorg. Synth.* **1966**, *8*, 211.

15) Hasenzahl, S.; Hausen, H.-D.; Kaim, W. *Chem. Eur. J.* **1995**, *1*, 95.

16) Spek, A. L. *PLATON, a multipurpose crystallographic tool*; Utrecht University: Utrecht, 1999.

17) Altomare, A.; Burla, M. C.; Camalli, M.; Cascarano, G. L.; Giacovazzo, C.; Guagliardi, A.; Moliterni, A. G. G.; Polidori, G.; Spagna, R. *J. Appl. Cryst.* **1999**, *32*, 115.

18) Sheldrick, G. M. *SHELXL-97, program for crystal structure refinement*; University of Göttingen: Germany, 1997.

19) Mitryaikina, M. A.; Gracheva, L. S.; Polovnyak, V. K.; Usachev, A. E.; Yablokov, Y. V. *J. Gen. Chem. USSR* **1992**, *62*, 821.

20) Imhoff, P.; van Asselt, R.; Elsevier, C. J.; Zoutberg, M. C.; Stam, C. H. *Inorg. Chim. Acta* **1991**, *184*, 73.

21) Delgado-Laita, E.; Sanchez-Muñoyerro, E. *Polyhedron* **1984**, *3*, 799.

22) Gillard, R. D.; Harrison, K.; Mather, I. H. *J. Chem. Soc., Dalton Trans.* **1975**, 133.

23) van der Poel, H.; van Koten, G.; Vrieze, K. *Inorg. Chim. Acta* **1981**, *51*, 241.

24) Morton, S.; Nixon, J. F. *J. Organomet. Chem.* **1985**, *282*, 123.

25) Mestroni, G.; Camus, A.; Zassinovich, G. *J. Organomet. Chem.* **1974**, *65*, 119.

26) Pahor, N. B.; Dreos-Garlatti, R.; Geremia, S.; Randaccio, L.; Tauzher, G.; Zangrando, E. *Inorg. Chem.* **1990**, *29*, 3437.

27) Mak, S.-T.; Yam, V. W.-W.; Che, C.-M.; Mak, T. C. W. *J. Chem. Soc., Dalton Trans.* **1990**, 2555.

28) Steinborn, D.; Ludwig, M. *J. Organomet. Chem.* **1993**, *463*, 65.

29) Collman, J. P.; Brauman, J. I.; Madonik, A. M. *Organometallics* **1986**, *5*, 310.

30) Gash, R. C.; Cole-Hamilton, D. J.; Whyman, R.; Barnes, J. C.; Simpson, M. C. *J. Chem. Soc., Dalton Trans.* **1994**, 1963.

31) Kleverlaan, C. J.; Stufkens, D. J.; Fraanje, J.; Goubitz, K. *Eur. J. Inorg. Chem.* **1998**, 1243.

32) Byers, P. K.; Canty, A. J.; Skelton, B. W.; White, A. H. *Organometallics* **1990**, *9*, 826.

33) Clark, R. J. H.; Dines, T. J. *Angew. Chem. Int. Ed. Engl.* **1986**, *25*, 131.

34) Rossenaar, B. D.; Stufkens, D. J.; Vlček, Jr., A. *Inorg. Chem.* **1996**, *35*, 2902.

35) Duling, D. R. *J. Magn. Res. Ser. B* **1994**, *104*, 105.

36) Aarnts, M. P.; Stufkens, D. J.; Vlček, Jr., A. *Inorg. Chim. Acta* **1997**, *266*, 37.

37) Kleverlaan, C. J.; Stufkens, D. J. *Inorg. Chim. Acta* **1999**, *284*, 61.

38) Nieuwenhuis, H. A.; van de Ven, M. C. E.; Stufkens, D. J.; Oskam, A.; Goubitz, K. *Organometallics* **1995**, *14*, 780.

39) Kleverlaan, C. J.; Stufkens, D. J. *J. Photochem. Photobiol. A: Chem.* **1998**, *116*, 109.